

Tert-butyl hydroperoxide decomposition as a descriptor for liquid-phase hydrocarbon oxidation over transition metal oxide-based catalysts: a screening study

Julia Büker,^a Jingqi Shang,^b Steven Angel,^c Eko Budiyanto,^d Harun Tüysüz,^d Hartmut Wiggers,^c Christof Schulz,^c Marcus Grünewald,^b Baoxiang Peng,^{*a,e} and Martin Muhler^{*a,e}

^a Laboratory of Industrial Chemistry, Ruhr University Bochum, Universitätsstr. 150, 44780 Bochum, Germany;

^b Lehrstuhl für Fluidverfahrenstechnik, Ruhr University Bochum, Universitätsstr. 150, 44780 Bochum, Germany;

^c EMPI, Institute for Energy and Materials Processes – Reactive Fluids and CENIDE, Center for Nanointegration Duisburg-Essen, University of Duisburg-Essen, Carl-Benz-Straße 199, 47057 Duisburg, Germany; ^d Department of Heterogeneous Catalysis, Max-Planck-Institut für Kohlenforschung, Kaiser-Wilhelm-Platz 1, 45470 Mülheim an der Ruhr, Germany; ^e Max Planck Institute for Chemical Energy Conversion, Stiftstraße 34-36, 45470

Mülheim an der Ruhr, Germany

Email: baoxiang.peng@techem.rub.de martin.muhler@ruhr-uni-bochum.de

Dedicated to Prof Graham Hutchings

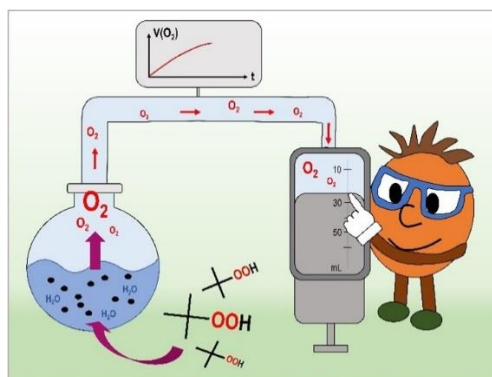
Received 12-22-2023

Accepted 03-22-2024

Published on line 03-27-2024

Abstract

Selective oxidation of hydrocarbons with environmentally friendly oxidizing agents is key to a sustainable future. Therefore, the development of heterogeneously catalyzed reactions using oxidants such as molecular oxygen and alkyl hydroperoxides is a promising approach. For the application of these oxidants on a large scale, highly active and selective catalysts must be developed, which requires a rapid screening of a large variety of materials. We report on a method that enables a volumetric quantification of the O₂ amount evolved from the decomposition of alkyl hydroperoxides, which serves as a fast initial screening step for identifying effective catalysts for hydrocarbon oxidation reactions.



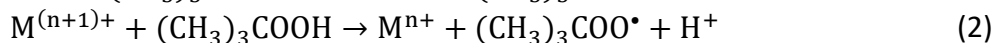
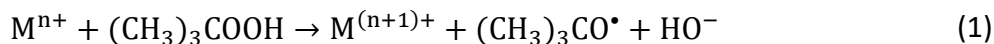
Keywords: Heterogeneous catalysis, liquid-phase oxidation, alkyl hydroperoxides, cobalt-based oxides, volumetric oxygen evolution

Introduction

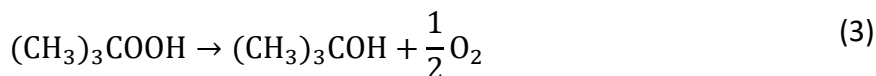
The selective oxidation of hydrocarbons is of high relevance for the chemical industry as it provides access to many fine chemicals of high value. A total annual capacity of close to 250×10^6 t organic chemicals are produced by oxidation, and approximately 50% of the production processes are carried out in the liquid phase.¹ However, many of the established liquid-phase oxidation processes are based on the use of stoichiometric oxidizing agents such as nitric acid and permanganates. Therefore, these processes suffer strongly from the formation of large quantities of environmentally harmful nitrous oxides or substantial amounts of inorganic solid waste as coupled products, which contribute to the production of environmental pollutants and climate change.² To overcome these sustainability issues, both academic and industrial research focus on the development of heterogeneously catalyzed reactions that offer the possibility of easy recovery and reuse of the involved catalyst. Especially, noble metal-based catalysts containing Pd, Pt and Au were extensively studied and showed high intrinsic activities, but due to their lower abundance and high costs, their use needs to be reconsidered.^{3–6} Thus, transition metal-based catalysts have raised much interest due to their favorable catalytic properties and higher resistance to poisoning, as well as their high thermal stability.⁷ Moreover, transition metal nanoparticles offer a large variety of catalytic properties, which are strongly determined by their partially filled d-bands.^{8,9} Due to the multiple possibilities to substitute different metals with various valences without changing the overall crystal structure, transition metal oxide catalysts of the spinel- or perovskite-type offer great potential for fine-tuning their properties to improve the established liquid-phase oxidation reactions.¹⁰ When analyzing their structure and correlating it to their catalytic properties, it is essential to consider the involved chemical elements, but also their oxidation state, the site occupation within the crystal structure, the spin state and coordinatively unsaturated sites at the surface.^{11,12}

Moreover, the use of environmentally benign oxidizing agents such as O_2 , H_2O_2 or *tert*-butyl hydroperoxide (TBHP) has raised much interest, since the formation of harmful waste can be reduced significantly. Among these oxidants, molecular O_2 is the most abundant and least expensive oxidizing agent providing the highest achievable atom efficiency of 50% for a one O atom transfer. The only by-product is H_2O , which leads to an optimal E-factor of 0.¹³ However, oxygen transfer into oxygenated products is strongly limited due to the high dissociation energy of O_2 and is additionally impeded kinetically by the positive free energy of the one-electron transfer to form O_2^- .^{13,14} In addition, the reaction of triplet paramagnetic O_2 with a typically singlet substrate molecule is forbidden according to quantum mechanical selection rules.¹⁴ As a result, most of the oxidation reactions with molecular O_2 proceed via one-electron processes induced by the formation of O_2^- superoxide or O_2^{2-} peroxide anions entering a radical chain mechanism in which a hydroperoxide is a key intermediate.¹⁵ Moreover, the reactivity of O_2 is restricted, and elevated pressures are required to increase its solubility and overcome mass transfer limitations.

As an alternative, peroxidic oxidants are promising candidates for liquid-phase oxidation reactions as they are liquid and highly soluble in suitable solvents. Among the peroxidic oxidants, H_2O_2 provides the highest atom efficiency of 47%, only forming H_2O as by-product. However, its rapid self-decomposition is often too fast to efficiently oxidize the reactant molecule. Thus, a large excess needs to be applied, which reduces the overall efficiency of the process and again increases its environmental impact. To overcome these drawbacks, alkyl hydroperoxides like TBHP can be used, which provide a higher thermal stability and selectivity.¹³ Nevertheless, its lower atom efficiency needs to be considered which is caused by the coupled formation of *tert*-butanol.¹³ TBHP is activated by a redox-active transition metal catalyst through its partial decomposition according to Equations 1 and 2, initiating the radical chain mechanism of a hydrocarbon oxidation reaction.¹⁶



Thus, an essential role of the applied catalyst is to effectively transform TBHP into highly reactive radicals that further oxidize the reactant molecules to oxygenated products. Therefore, information about the peroxide decomposition ability of a catalyst is of high importance when searching for suitable catalysts for the heterogeneously catalyzed oxidation of hydrocarbons using alkyl hydroperoxides. However, if no reactant is present, TBHP is unselectively decomposed into *tert*-butanol and O₂, where the amount of the latter can be determined volumetrically and provides information on the activity of the catalyst (Equation 3).



Moreover, alkyl hydroperoxides are formed during hydrocarbon oxidation reactions as key intermediates which also need to be decomposed catalytically to form the desired final products.¹⁵ Therefore, TBHP can also be a suitable reactant to mimic the decomposition ability of a catalyst towards the formed intermediate alkyl hydroperoxides, for example, when using an alternative oxidizing agent such as O₂.¹²

In this work, we report on an efficient method to rapidly screen the activity of various transition metal-based catalysts of the spinel- or perovskite-type for oxidation reactions with regard to their alkyl hydroperoxide decomposition ability by performing the decomposition of TBHP in a batch reactor with volumetric determination of the amount of evolved O₂ as a function of time. This quantitative method helps to achieve a quick overview of the TBHP decomposition activity of a large variety of catalysts without having to perform the laborious oxidation reactions, serving as an initial screening step in the development of highly active and selective catalysts for hydrocarbon oxidation reactions.

Results and Discussion

To assess the reproducibility of the volumetric measurements of the evolved O₂ amounts, TBHP decomposition over a commercial CoFe₂O₄ catalyst was performed four times under standard reaction conditions, which resulted in nearly equal curves with a high accuracy of ±2.4% (Figure S2). Mass transfer limitations were excluded by varying the stirring speed during the decomposition reaction between 200 and 800 rpm under otherwise standard reaction conditions (Figure S3). While the evolved O₂ amount over time increased gradually with increasing stirring speed up to 600 rpm, similar results within the standard deviation were recorded at 700 and 800 rpm. These results indicate that mass transport limitations can be excluded when stirring with a speed of 700 rpm, whereas slower stirring limits the reaction rate due to a too slow mass transport in the three-phase system. Therefore, a stirring speed of at least 700 rpm needs to be applied for reliable results.

The TBHP decomposition experiments provide useful information about the kinetics of the decomposition reaction. Figure S4 shows the evolved O₂ amounts during TBHP decomposition over commercial CoFe₂O₄ as a function of time, using different catalyst amounts between 30 and 70 mg. As expected, the reaction rate linearly increased with increasing catalyst amount up to 60 mg, which can be explained by the linear increase of the number of exposed active sites in the reaction volume for the TBHP decomposition reaction. However, a lower increase than expected was recorded for the reaction using 70 mg catalyst, which indicates the onset of mass transport limitations.

Moreover, the volumetric experiments enable the determination of the reaction order of the TBHP decomposition reaction by performing the decomposition using different initial TBHP amounts between 200 and 700 μL , which corresponds to a TBHP concentration in acetonitrile of 0.10 and 0.36 mol L^{-1} , respectively (Figure 1). The linearized plot of the obtained reaction rates as a function of the initial TBHP concentration resulted in a straight line with a slope of 1.2 indicating first-order reaction kinetics for the TBHP decomposition over a commercial CoFe_2O_4 catalyst at 60 °C with a high accuracy of $R^2 = 0.991$, which is in accordance with other findings in literature.¹⁷⁻¹⁹

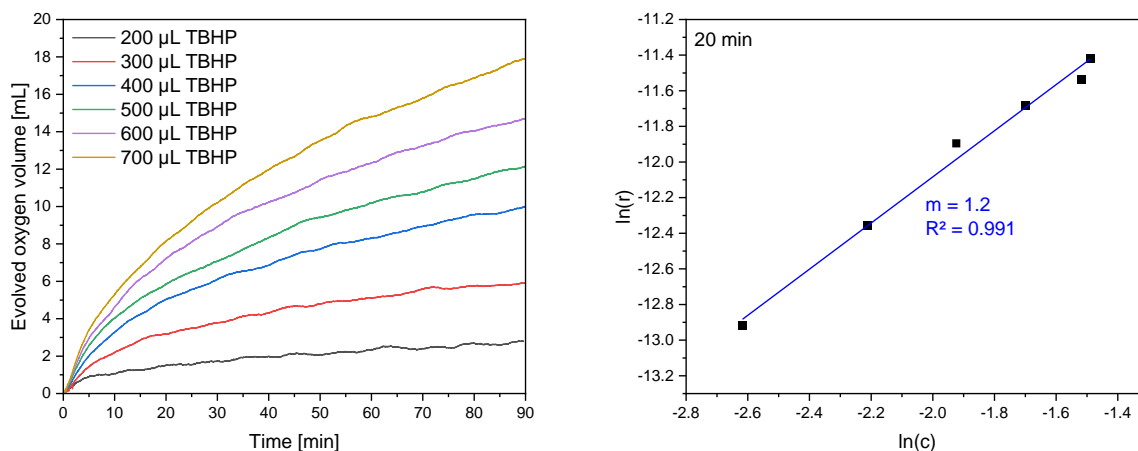


Figure 1. Evolved O_2 volumes as a function of time for TBHP decomposition experiments using different initial TBHP concentrations (left) and the corresponding linearized plot of the reaction rate as a function of the initial TBHP concentration after 20 min (right). Reaction conditions: 50 mg commercial CoFe_2O_4 , 20 mL acetonitrile, 200/300/400/500/600/700 μL TBHP, 60 °C, 700 rpm.

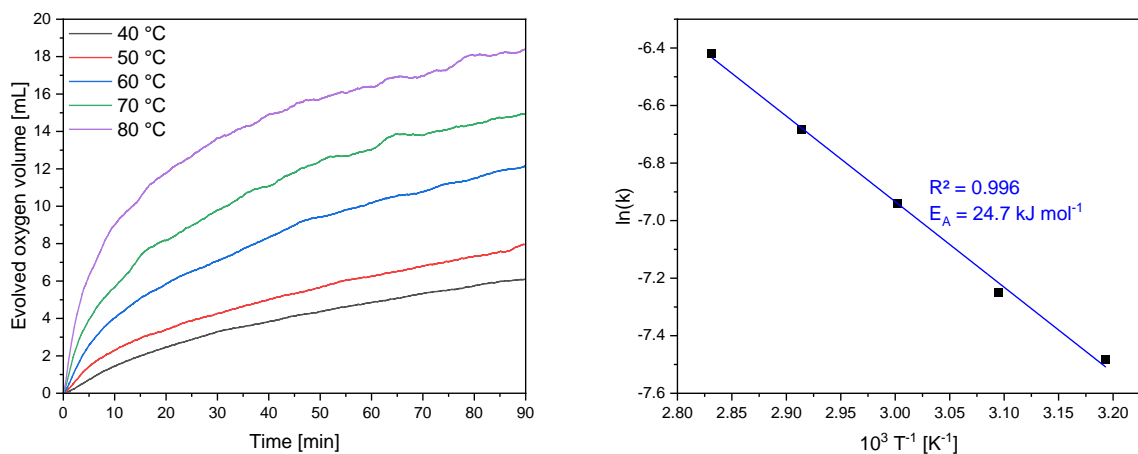


Figure 2. The evolved O_2 volumes as a function of time for TBHP decomposition experiments at different temperatures (left) and the corresponding Arrhenius plot (right). Reaction conditions: 50 mg commercial CoFe_2O_4 , 20 mL acetonitrile, 500 μL TBHP, 40/50/60/70/80 °C, 700 rpm.

Based on this knowledge, the apparent activation energy of TBHP decomposition over CoFe_2O_4 can be determined performing temperature variation experiments (Figure 2). The amount of evolved O_2 increased gradually with increasing temperature between 40 and 80 °C. The linearization of the data based on first-order

reaction kinetics is well-suited for an Arrhenius plot resulting an apparent activation energy of 24.7 kJ mol⁻¹ with a high accuracy of $R^2 = 0.996$ (Figures 2 and S5). In comparison, Qi *et al.* found apparent activation energies between 59 and 142 kJ mol⁻¹ when investigating the decomposition of TBHP over birnessite-type manganese oxides.¹⁹

Moreover, the stability and reusability of the catalysts under the respective reaction conditions can be tested in the volumetric measurement set-up by applying the same catalyst several times in the same reaction. We performed TBHP decomposition three consecutive times under standard reaction conditions over the commercial CoFe₂O₄ catalyst and found a decrease in the catalytic activity of about 25% (Figure S6). However, the direct comparison of the evolved O₂ volume is not valid in this case, as the catalyst was not fully recovered after each reaction run. Therefore, the comparison of the obtained reaction rates is more reliable, which indicates a decrease in catalytic activity after the first reaction run, whereas an equal reaction rate was obtained in the second and third reaction run, respectively. This observation indicates an initial loss of activity over the commercial CoFe₂O₄ catalyst, which afterwards enables a constant degree of conversion.

In addition, the effect of the solvent was investigated on the TBHP decomposition over CoFe₂O₄ (Figure S7). It becomes clear that acetonitrile is the most suitable solvent for the decomposition reaction, which has been reported for many reactions where TBHP was involved. It is preferred due to its highly polar, but aprotic nature.^{17,20} Consequently, the use of acetone and cyclohexane as aprotic solvents was also successful but led to a lower amount of evolved O₂. The protic aromatic benzyl alcohol can also be a suitable alternative for oxidation reactions using TBHP as oxidant, while protic solvents such as H₂O, methanol, ethanol and 2-propanol strongly inhibited the decomposition reaction.²¹ The possibility of whether highly reactive species are formed by the reaction of TBHP with the solvents is currently being studied too. Electron paramagnetic resonance spectroscopy is the method of choice to investigate the potentially formed radicals, results of which will be disclosed in other research outputs from our group.

On the one hand, the volumetric gas measurement set-up can provide kinetic information on the TBHP decomposition reaction. On the other hand, a fast screening of suitable catalysts needs to be established to compare their relative activity to significantly speed up the development of suitable catalysts for oxidation reactions with TBHP as oxidant. Therefore, a large comparative study including 42 catalysts was performed comparing the reaction rate of TBHP decomposition under similar reaction conditions after 60 min (Figure 3). Obviously, transition metal-based catalysts of the perovskite-type (red) are much more active towards TBHP decomposition compared with spinel catalysts (green). In addition, clear trends of the catalytic activity can be observed for all catalyst series. For example, TBHP decomposition experiments over a series of Co_{3-x}Fe_xO₄ spinel catalysts with varying Fe contents verified CoFe₂O₄ to be the most active catalyst. This assumption was also confirmed when using H₂O₂ as peroxidic oxidant, and a similar volcano trend was observed for the aerobic oxidation of cyclohexene, indicating that the decomposition reaction of TBHP is also valid to mimic the decomposition of the *in situ* formed hydroperoxides within hydrocarbon oxidation reactions.¹²

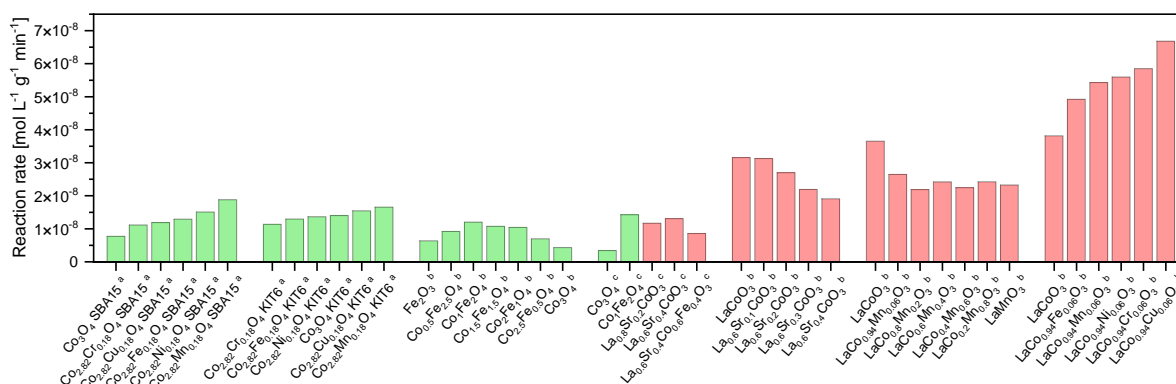


Figure 3. The reaction rates of TBHP decomposition over a variety of transition metal oxide catalysts as a function of catalyst composition. Catalysts of the spinel-type are shown in green, and perovskites in red. Reaction conditions: 50 mg spinel or 20 mg perovskite catalyst, 20 mL acetonitrile, 500 μL TBHP, 60 $^{\circ}\text{C}$, 700 rpm, 60 min. The catalysts were synthesized using a nanocasting method,^a spray-flame synthesis^b or were supplied by Merck^c.

Moreover, a series of metal-doped $\text{Co}_{2.82}\text{M}_{0.18}\text{O}_4$ spinel catalysts, synthesized by a nanocasting method using SBA-15 as template, showed an increasing activity when substituting Co by Cr, Cu, Fe, Ni and Mn. However, a similar spinel series with KIT-6 as the template²² led to different activities, with Cr being the least active metal, while the insertion of Mn into the spinel structure again provided the highest reaction rate. Thus, not only the chemical composition, but also the mesoporous structure of the catalyst has a significant influence on the catalytic activity.

While the incorporation of Mn into the Co_3O_4 spinel structure enhanced the catalytic activity towards TBHP decomposition, Mn substitution into LaCoO_3 was already detrimental at low doping levels and led to a significant decrease of the reaction rate. Thus, it has to be taken into account that the catalytic behavior of transition metal oxide-based catalysts strongly depends on their structure, and the substitution of presumably highly active metal ions may lead to a drastic decrease of the catalytic activity.

LaCoO_3 was also the most active sample for TBHP decomposition within a series of $\text{La}_{1-x}\text{Sr}_x\text{CoO}_3$ perovskites, where the La^{3+} cations were substituted by Sr^{2+} aiming at the creation of highly active oxygen vacancies.²³ However, Sr contents up to 10% did not affect the catalytic activity, whereas higher Sr concentrations led to a gradual decrease of the decomposition reaction rate. Importantly, the catalytic activity of three comparable LaCoO_3 samples, synthesized by spray-flame synthesis under similar reaction conditions, only deviated slightly, which again confirms the high reliability of the volumetric measurements, as well as of the synthesis method.

While the substitution of metal ions into the perovskite structure decreased the reaction rate of TBHP decomposition, doping of metals within a $\text{LaCo}_{0.94}\text{M}_{0.06}\text{O}_3$ perovskite series led to a significant increase of the catalytic activity following the sequence $\text{Fe} < \text{Mn} < \text{Ni} < \text{Cr} < \text{Cu}$. $\text{LaCo}_{0.94}\text{Cu}_{0.06}\text{O}_3$ was found to be the most active catalyst for TBHP decomposition within the investigated catalyst series. Thus, this comparative study on TBHP decomposition in a volumetric measurement set-up demonstrates this method to be highly suitable to quickly screen the decomposition ability of various catalysts towards alkyl hydroperoxides, which can be used as environmentally benign oxidizing agents for the selective oxidation of hydrocarbons.

Conclusions

Replacing hazardous oxidants with environmentally more benign oxidizing agents such as alkyl hydroperoxides is key to the development of new efficient synthesis routes for oxygenated products. *Tert*-butyl hydroperoxide is a promising alkyl hydroperoxide for oxidation reactions due to its high thermal stability. It needs to be decomposed over a suitable catalyst into reactive radicals which then initiate the radical chain mechanism of hydrocarbon oxidation reactions. Thus, a highly active and selective catalyst is needed to achieve the heterogeneously catalyzed oxidation using alkyl hydroperoxides as oxygen source. A broad variety of catalysts must be investigated which results in a significant time-consuming effort when performing the oxidation reactions in the liquid phase. To overcome this hurdle, we present a fast method to investigate the decomposition ability of transition metal-based catalysts of the spinel- or perovskite-type towards *tert*-butyl hydroperoxide by recording the evolved O₂ amounts in a volumetric set-up as a function of time. This method enables a faster investigation of large series of catalysts and serves as an initial screening step for identifying effective catalysts for hydrocarbon oxidations with alkyl hydroperoxides. The evolved O₂ volumes, measured against time during the decomposition of *tert*-butyl hydroperoxide, were found to vary strongly as a function of the chemical composition and structure of the catalysts, rendering the O₂ evolution rate a suitable descriptor for the activity of the respective catalyst. In addition, the stability of the catalysts can be studied, as well as the effect of the used solvent. Moreover, the volumetric measurements can provide kinetic information on the alkyl hydroperoxide decomposition reaction by investigating the effects of the catalyst amount, the reactant concentration and the reaction temperature. This is highly useful information when studying the overall hydrocarbon oxidation reaction as it allows to separate the complex oxidation reaction network into different parts.

Experimental Section

General. TBHP decomposition experiments were carried out in a commercial set-up (GASMESS-5 supplied by MesSen Nord GmbH, Figure S1). Figure 4 shows a scheme of the volumetric gas measurement device equipped with a round-bottom flask which is connected to a reflux condenser to avoid the loss of the reaction mixture by evaporation. The solvent and the respective catalyst are added to the flask and heated to a suitable temperature by an oil bath. The resulting suspension is stirred continuously, and the actual reaction is started by adding TBHP rapidly to the flask which is then quickly sealed by a plug. A differential pressure gauge measures the pressure difference relative to ambient pressure, which is recorded by an electronic device. A constant pressure is secured by the facile movement of a piston syringe.

The degree of TBHP conversion is calculated according to Equation 4, where X_t is the conversion at time t , $V_{O_2,rec}$ is the recorded evolved O₂ volume, and $V_{O_2,total}$ is the total O₂ volume which could be evolved at full conversion. $V_{O_2,total}$ is derived using the ideal gas law, where n is the molar amount, R is the gas constant, T is the temperature and p the pressure. Note that conversions are only comparable in case of equal reaction conditions.

$$X_t = \frac{V_{O_2,rec}}{V_{O_2,total}} = \frac{V_{O_2,rec} p}{\frac{1}{2} n_{TBHP} R T} \cdot 100 \quad (4)$$

Moreover, the mass- and surface-normalized reaction rates can be derived using Equations 5 and 6, which enable the direct comparison of the reaction rates achieved by different catalysts under deviating reaction conditions. The concentration of TBHP in the reaction solution is abbreviated as c_{TBHP} , while m_{cat} , t and S_{BET} are the catalyst mass, time and specific surface area of the catalyst, respectively.

$$r_{\text{mass-normalized}} = \frac{c_{\text{TBHP}} \frac{X_t}{100}}{m_{\text{cat}} t} \quad (5)$$

$$r_{\text{surface+mass-normalized}} = \frac{c_{\text{TBHP}} \frac{X_t}{100}}{m_{\text{cat}} t S_{\text{BET}}} \quad (6)$$

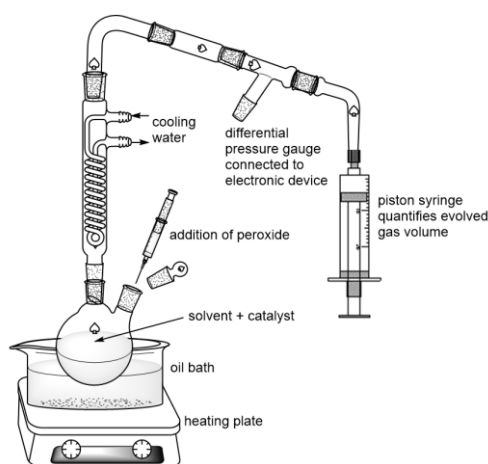


Figure 4. Scheme of the volumetric gas measurement set-up showing the flask in which the catalyst and solvent had been filled before the respective peroxide was added and the volumetric measurement was started. Loss of the solvent was prevented by a reflux condenser. The evolved gas was quantified by measuring the internal pressure via a differential pressure gauge, and pressure was kept constant by the automatized movement of the piston syringe.

Commercial CoFe_2O_4 , Co_3O_4 , $\text{La}_{0.8}\text{Sr}_{0.2}\text{CoO}_3$, $\text{La}_{0.6}\text{Sr}_{0.4}\text{CoO}_3$ and $\text{La}_{0.6}\text{Sr}_{0.4}\text{Co}_{0.6}\text{Fe}_{0.4}\text{O}_3$ catalysts were obtained from Merck. Two series of $\text{Co}_{2.82}\text{M}_{0.16}\text{O}_4$ spinel catalysts with $\text{M} = \text{Co}, \text{Cr}, \text{Cu}, \text{Fe}, \text{Ni}, \text{Mn}$ were synthesized using a nanocasting method with KIT-6- and SBA-15-ordered mesoporous silica as templates. The detailed procedure is described elsewhere.²² $\text{Co}_x\text{Fe}_{3-x}\text{O}_4$ spinel catalysts and a series of $\text{La}_{1-x}\text{Sr}_x\text{CoO}_3$, perovskite catalysts were synthesized by spray-flame synthesis. The detailed synthesis procedure for these catalysts is described elsewhere.^{12,18} A series of $\text{LaCo}_{1-x}\text{Mn}_x\text{O}_3$ nanoparticles was synthesized via spray-flame synthesis. For the preparation of the precursor solution, the corresponding masses of $\text{La}(\text{NO}_3)_3$, $\text{Co}(\text{NO}_3)_3$ and $\text{Mn}(\text{NO}_3)_2$ were dissolved in a solvent mixture of 35 vol.% ethanol and 65 vol.% 2-ethylhexanoic acid. The total metal concentration was kept at 0.2 mol L^{-1} . The syntheses were carried out in spray flame placed in a reaction chamber at a pressure of 970 mbar. The precursor solutions were injected via syringe pumps to a capillary of an external-mixing two-fluid nozzle at a constant flow rate of 2 mL min^{-1} and atomized with 10 slm (standard liters per minute) of oxygen used as dispersion gas. A premixed pilot flame (methane and oxygen, 2.5 and 16 slm, respectively) was used to ignite and stabilize the spray flame. A coaxial sheath gas flow was set to 140 slm, while an additional quench gas flow downstream the reaction chamber was set to 230 slm. To remove adsorbed water and combustion residuals from the as-prepared catalyst surface, each sample was calcined in a tube furnace at

250 °C for 2 h with an air flow rate of 500 L h⁻¹. A series of LaCo_{0.94}M_{0.06}O₃ (M = Co, Cr, Cu, Fe, Ni, Mn) perovskites was synthesized under similar reaction conditions using La(NO₃)₃, Co(NO₃)₃ and the corresponding metal nitrates as precursors.

The TBHP decomposition reaction was carried out in the peroxide decomposition setup (Gasmess-5, Figures 4 and S1). As standard conditions, 50 mg catalyst were dispersed in 20 mL acetonitrile in a 25 mL round-bottom flask using an ultrasonic bath for 2 min. The flask was transferred to the reaction set-up and the solution was heated to 60 °C and stirred at 700 rpm. 500 µL TBHP were added, the gas volume measurement was started immediately and the decomposition reaction was run for 90 min. Deviations from the standard procedure are mentioned in the figure captions.

Acknowledgements

This research was funded by the Deutsche Forschungsgemeinschaft (DFG, German Research Foundation) in the framework of the Collaborative Research Center / Transregio “Heterogeneous Oxidation Catalysis in the Liquid Phase”-388390466-TRR 247 (Projects A1, C1, C2). The work was supported by the “Center for Solvation Science (ZEMOS)” funded by the German Federal Ministry of Education and Research (BMBF) and by the Ministry of Culture and Research of North Rhine-Westphalia.

Supplementary Material

Supplementary Material is available via the journal website.

References

1. Teles, J. H.; Hermans, I.; Franz, G.; Sheldon, R. A. in *Ullmann's Encyclopedia of Industrial Chemistry*, Wiley, 2010; pp 1–103.
2. Yu, H.; Peng, F.; Tan, J.; Hu, X.; Wang, H.; Yang, J.; Zheng, W. *Angew. Chem. Int. Ed.* **2011**, *17*, 4064–4068. <https://doi.org/10.1002/ange.201007932>
3. Dimitratos, N.; Villa, A.; Bianchi, C. L.; Prati, L.; Makkee, M. *Appl. Catal. A.* **2006**, *311*, 185–192. <https://doi.org/10.1016/j.apcata.2006.06.026>
4. Dimitratos, N.; Lopez-Sanchez, J. A.; Hutchings, G. J. *Chem. Sci.* **2012**, *3*, 20–44. <https://doi.org/10.1039/C1SC00524C>
5. Cai, Z.-Y.; Zhu, M.-Q.; Dai, H.; Liu, Y.; Mao, J.-X.; Chen, X.-Z.; He, C.-H. *Adv. Chem. Eng. Sci.* **2011**, *1*, 15–19. <http://dx.doi.org/10.4236/aces.2011.11003>
6. Ameer, N.; Bedrane, S.; Bachir, R.; Choukchou-Braham, A. *J. Mol. Catal. A: Chem.* **2013**, *374*, 1–6. <https://doi.org/10.1016/j.molcata.2013.03.008>
7. Rao, C. N. R.; Raveau, B.; *Transition metal oxides*, Wiley-VCH, 1998. ISBN: 978-0-471-18971-8.
8. Gawande, M. B.; Pandey, R. K.; Jayaram, R. V. *Catal. Sci. Technol.* **2012**, *2*, 1113–1125. <https://doi.org/10.1039/c2cy00490a>
9. Védrine, J. C. *Catalysts* **2017**, *7*, 341. <https://doi.org/10.3390/catal7110341>

10. Kung, H. H. in *Studies in Surface Science and Catalysis*, Elsevier, **1989**, pp. 6–26.
[https://doi.org/10.1016/S0167-2991\(08\)60231-1](https://doi.org/10.1016/S0167-2991(08)60231-1)
11. Zasada, F.; Grybos, J.; Indyka, P.; Piskorz, W.; Kaczmarczyk, J.; Sojka, Z. *J. Phys. Chem. C* **2014**, *118*, 19085–19097.
<https://doi.org/10.1021/jp503737p>
12. Büker, J.; Angel, S.; Salamon, S.; Landers, J.; Falk, T.; Wende, H.; Wiggers, H.; Schulz, C.; Muhler, M.; Peng, B. *Catal. Sci. Technol.* **2022**, *12*, 3594–3605.
<https://doi.org/10.1039/D2CY00505K>
13. Strukul, A. S. G. in *Liquid Phase Oxidation via Heterogeneous Catalysis. Organic Synthesis and Industrial Applications*, Wiley: Hoboken, 2013, pp 1–20.
14. Büker, J.; Muhler, M.; Peng, B. *ChemCatChem* **2023**, *15*, e202201216.
<https://doi.org/10.1002/cctc.202201216>
15. Büker, J.; Peng, B. *Mol. Catal.* **2022**, *525*, 112367.
<https://doi.org/10.1016/j.mcat.2022.112367>
16. Olah, G. A.; Molnár, Á. *Hydrocarbon chemistry*, John Wiley & Sons, 2003.
17. Waffel, D.; Alkan, B.; Fu, Q.; Chen, Y.-T.; Schmidt, S.; Schulz, C.; Wiggers, H.; Muhler, M.; Peng, B. *ChemPlusChem* **2019**, *84*, 1155–1163.
<https://doi.org/10.1002/cplu.201900429>
18. Turrà, N.; Neuenschwander, U.; Baiker, A.; Peeters, J.; Hermans, I. *Chemistry* **2010**, *16*, 13226–13235.
<https://doi.org/10.1002/chem.201000489>
19. Qi, L.; Qi, X.; Wang, L.; Feng, L.; Lu, S. *Catal. Commun.* **2014**, *49*, 6–9.
<https://doi.org/10.1016/j.catcom.2014.01.028>
20. Chàvez, J. E.; Crotti, C.; Zangrando, E.; Farnetti, E. *J. Mol. Catal. A: Chem.* **2016**, *421*, 189–195.
<https://doi.org/10.1016/j.molcata.2016.05.023>
21. Cao, Y.; Yu, H.; Wang, H.; Peng, F. *Catal. Commun.* **2017**, *88*, 99–103.
<https://doi.org/10.1016/j.catcom.2016.10.002>
22. Falk, T.; Budiyo, E.; Dreyer, M.; Büker, J.; Weidenthaler, C.; Behrens, M.; Tüysüz, H.; Muhler, M.; Peng, B. *ACS Appl. Nano Mater.* **2022**, *5*, 17783–17794.
<https://doi.org/10.1021/acsnm.2c03757>
23. Büker, J.; Alkan, B.; Chhabra, S.; Kochetov, N.; Falk, T.; Schnegg, A.; Schulz, C.; Wiggers, H.; Muhler, M.; Peng, B. *Chem. Eur. J.* **2021**, *27*, 16912–16923.
<https://doi.org/10.1002/chem.202103381>

This paper is an open access article distributed under the terms of the Creative Commons Attribution (CC BY) license (<http://creativecommons.org/licenses/by/4.0/>)